The role of the host–guest interactions in the relative stability of compressed encapsulated homodimers and heterodimers of amides and carboxylic acids

ARTICLE *in* THEORETICAL CHEMISTRY ACCOUNTS · JULY 2014

Impact Factor: 2.23 · DOI: 10.1007/s00214-014-1503-8

5 AUTHORS, INCLUDING:

Demeter Tzeli
National Hellenic Research Foundation
52 PUBLICATIONS **502** CITATIONS
SEE PROFILE

Ioannis D Petsalakis
National Hellenic Research Foundation
142 PUBLICATIONS **1,590** CITATIONS
SEE PROFILE

Theor Chem Acc (2014) 133:1503
DOI 10.1007/s00214-014-1503-8

REGULAR ARTICLE

The role of the host–guest interactions in the relative stability of compressed encapsulated homodimers and heterodimers of amides and carboxylic acids

Demeter Tzeli · Ioannis D. Petsalakis · Giannoula Theodorakopoulos · Dariush Ajami · Julius Rebek Jr.

Received: 14 November 2013 / Accepted: 8 May 2014

Abstract A theoretical study has been carried out on the encapsulation of heterodimers and homodimers of *p*-methylbenzoic acid, *p*-ethylbenzoic acid, *p*-methylbenzamide, and *p*-ethylbenzamide molecules in reversible capsules with a very limited cavity. The drastic compression of the guests in the capsules has been studied by density functionally theory employing the M06-2X and ωB97X-D functionals with the 6-31G(d,p) basis set following preliminary calculations by the fast ONIOM[M06-2X/6-31G(d,p):PM6] methodology. Both functionals are in agreement with respect to the geometry, the interaction energies between the monomers and the relative ordering of the isomers. We found that encapsulation is favorable even for the larger *p*-ethyl compounds, but complexes of encapsulated dimers lie more than 4 kcal/mol above complexes with two non-interacting encapsulated monomers. The monomers prefer to be by themselves in the host. This is the reason why the present encapsulated dimers have not been found experimentally. The relative stability of the encapsulated complexes is reversed compared to complexes in a large cavity (Tzeli et al. in J Am Chem Soc 133:16977, 2012). This shows the possibility of separation of competitive guests via reversible encapsulation under appropriate conditions.

Keywords DFT calculations · Encapsulation · Hydrogen bonding · Compression · Carboxylic acid · Amide

1 Introduction

The study of the intermolecular interactions within supramolecular systems has become a very active area of research over the last five decades due to their important role in nature [1], i.e., multiple weak interactions between molecules provide enzymes with the ability to direct reactions to specific substrates, at specific sites of these substrates. The supramolecular interactions form "the core" of molecular recognition, regioselectivity, enantioselectivity, and shape selectivity in enzymatic reactions. Thus, many experimental and theoretical studies have been carried out regarding hydrogen bonding, van der Waals attractions, dipole–dipole interactions, steric repulsions, ion pairing, and other weak forms of bonding [1–4]. In the vast effort that has been done toward understanding supramolecular chemistry, many host–guest systems have been synthesized that exhibit remarkable properties [1–8].

Cages are unique among synthetic molecular receptors because of their encapsulation properties [5–8]. A wide range of guests of different shape, size, and charge have been trapped within cages on a timescale that ranges from microseconds to forever [9]. Desired features of the capsules comprise selectivity in guest encapsulation, control of guest orientation and dynamics within the cage, and reversibility, which allows guest uptake and release under

Electronic supplementary material The online version of this article (doi:10.1007/s00214-014-1503-8) contains supplementary material, which is available to authorized users.

D. Tzeli (✉) · I. D. Petsalakis · G. Theodorakopoulos (✉)
Theoretical and Physical Chemistry Institute, National Hellenic Research Foundation, 48 Vassileos Constantinou Ave., 116 35 Athens, Greece
e-mail: dtzeli@eie.gr

G. Theodorakopoulos
e-mail: ithe@eie.gr

D. Ajami · J. Rebek Jr.
Department of Chemistry, Skaggs Institute for Chemical Biology, The Scripps Research Institute, 10550 North Torrey Pines Road, La Jolla, CA 92037, USA

Published online: 31 May 2014

controlled conditions [9]. As a result, many potential applications can be envisioned for molecular containers, ranging from drug release to catalysis [10] and memory storage devices [11]. The central issue of their preparation has been tackled both via covalent synthesis and, more recently, via self-assembly [12–14].

Self-assembly encapsulation is based on the capsule components bearing complementary functional groups capable of reversible non-covalent interactions, which are usually hydrogen-bonding interactions. They facilitate reversibility and reliable directionality, and they offer great plasticity and fast equilibration. The encapsulation of guest molecules is dependent on the complementarity of the size, the shape, the location of functional groups, and the flexibility of the guest as well as the chemical surface of the host cavity [15, 16].

Observation of individual hydrogen-bonded dimers in solution is difficult because of their short lifetimes and the rapid exchange of partners, but reversible encapsulation allows the temporary isolation of the guest dimers by mechanical barriers and their characterization by NMR methods at normal conditions [17–19]. Recently, the relative stability of encapsulated homodimers and heterodimers of amides, boronic acids, and carboxylic acids in capsules with sufficiently large cavities for the dimers has been examined both experimentally by NMR [17, 19] and theoretically via density functional theory (DFT) [20–22]. Experiment and theory determine the % distribution of the encapsulated dimers in good agreement, and it is shown that the size of the cage affects the % distribution [20–22]. When the capsule was large enough to accommodate the dimers without any significant compression, the dimerization energy ordering of encapsulated dimers was found to be practically the same as that in the gas phase [15, 20–22]. In smaller cages where however the dimers fit well in the cage, hydrogen-bonding interactions of the amide segments with the cage are formed and the hydrogen bonds in the corresponding dimers are weakened resulting in lower dimerization energy and different % distribution from those in the larger cage and the free dimers [19, 22]. However, in all above cases, no compression of the dimers, in terms of distortions of the dimer geometry, was observed.

Encapsulation and compression of different carboxylic acid dimers has been described both experimentally in the **1.2$_4$.1** cage [18] and theoretically in three cages of different size and stability [23]. A shortening of the hydrogen bonds in the compressed dimer was observed experimentally, and the effects of encapsulation were compared to the effect of external pressure on the hydrogen bond geometries of carboxylic acid dimers in the solid state [18]. In the theoretical study, the shortening of the hydrogen bonds was not reproduced but attractive interactions between the guests and the walls of the capsules were found, responsible for the stabilization of the complexes for all the cases including those in which the dimers do not fit very well [23]. In view of the earlier work on competitive encapsulated dimers [20–22], a question arises regarding the relative stability of competitive hydrogen-bonded homodimers and heterodimers in a capsule whose cavity is not spacious enough for the encapsulated dimers, such as the **1.1** cage employed previously [23]. Another question is why none of the present encapsulated dimers have been found experimentally in the short capsule **1.1**. Furthermore, it is of interest to consider whether it is possible to separate competitive dimers or monomers via encapsulation.

In the present study, theoretical DFT calculations are employed in order to determine the effect of a cage with a very limited cavity employed for encapsulation of antagonistic dimers of similar size on their relative stability and on their geometry. Preliminary calculations employing the ONIOM methodology have been carried out, which, in addition, offer information on the efficacy of the fast ONIOM method for compressed systems.

2 Computational details

Heterodimers and homodimers of *p*-methylbenzoic acid (**C$_M$**), *p*-ethylbenzoic acid (**C$_E$**), *p*-methylbenzamide (**A$_M$**), and *p*-ethylbenzamide (**A$_E$**) are computed in the gas phase and as guests in the self-assembly capsule **1.1**. Cage **1.1** [24] consists of two cavitands **1**, see Fig. 1. The free dimers are also depicted in Fig. 1, while the encapsulated structures are presented in Fig. 2 for both methyl- and ethyl-substituted benzamide dimers, in Fig. 3 for both substituted benzoic acid dimers, and in Fig. 4 for both substituted benzamides–benzoic acids dimers. The encapsulated complexes are named here with the name of the capsule followed by the abbreviation of the dimer and a number that shows the relative ordering of the isomer, for example, **1.1_AA$_M$-1**: lowest minimum structure (−1) of encapsulated *p*-methylbenzamide homodimer (**AA$_M$**) in the **1.1** cage. Homodimers of *p*-methylbenzoic acid and *p*-ethylbenzoic acid in the **1.1** and **1.2$_4$.1** cages have been also calculated previously at the M06-2X/6-31G(d,p) level of theory [23].

All calculated structures were fully optimized by DFT calculations using the M06-2X [25, 26] and the ωB97X-D [27] functionals in conjunction with the 6-31G(d,p) basis set [28]. The M06-2X functional is a hybrid meta-exchange correlation functional; the ωB97X-D functional includes 100 % long-range exact exchange, a small fraction of short-range exact exchange, a modified B97 exchange density functional for short-range interaction, and empirical dispersion corrections. It has been found that the M06-2X/6-31G(d,p) level of theory predicts well the dimerization energies of heterodimers and homodimers of amides

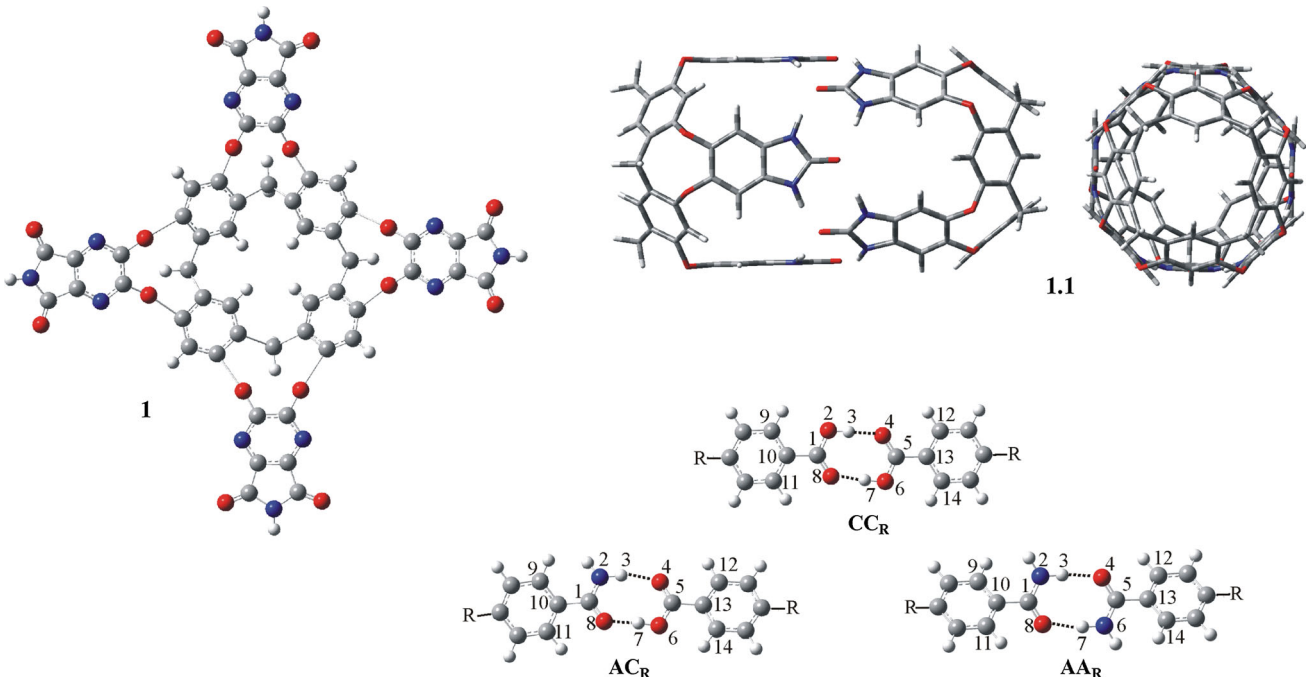

Fig. 1 Cavitands **1**, capsule **1.1** viewed from two different angles, i.e., along the central axis of the capsule and end-on view, and substituted benzamide ($\mathbf{A_R}$) and benzoic acid ($\mathbf{C_R}$) homodimers and heterodimers of amide and carboxylic acid with R = methyl and ethyl group. (H atoms = *white spheres*, C = *gray spheres*, O = *red spheres*, and N = *blue spheres*)

and carboxylic acids compared to the ab initio methods MP2/aug-cc-pVQZ and CCSD(T)/aug-cc-pVTZ [21]. The ωB97X-D functional yields satisfactory accuracy for non-covalent interactions and long-range interactions compared to other functionals and to the MP2/aug-cc-pVTZ and CCSD(T)/aug-cc-pVTZ levels of theory [27, 29]. The effect of inclusion of diffuse functions was examined by M06-2X/6-311+G(d,p) calculations, and it was found to be not significant for the encapsulated dimers (see below), considering the great increase in computational effort involved. The above full-DFT calculations followed preliminary calculations employing the fast ONIOM methodology [30–32], where the systems were defined as two regions (layers). The high layer consists of the guests calculated at the M06-2X/6-31G(d,p) level of theory, and the low layer is the capsule calculated at the PM6 level of theory. Note that the present ONIOM calculations are about 30 times faster than the corresponding DFT calculations, and therefore, it is of interest to examine its applicability for the present systems, where the dimers are compressed inside the capsule and they adopt a different arrangement in the limited space of the capsule compared to the corresponding free dimers.

All interaction energies and dimerization energies presented here have been corrected with respect to the basis set superposition error (BSSE) via the counterpoise procedure [33, 34]. In the case of the ONIOM method, the BSSE correction was taken into account for the dimerization energies of the encapsulated dimers. All calculations were carried out using the Gaussian 09 program [35].

3 Results and discussion

3.1 Free dimers

The free heterodimers and homodimers of *p*-methyl- and *p*-ethyl-substituted amide and carboxylic acids are depicted in Fig. 1. Selected bond distances, angles, and dihedral angles of the free dimers along with dimerization energies are given in Table 1. The two levels of theory, M06-2X/6-31G(d,p) and ωB97X-D/6-31G(d,p), predict the same geometries with the exception of the hydrogen bond length of the carboxylic homodimers, where the ωB97X-D/6-31G(d,p) level predicts elongated hydrogen bond distances by 0.07 Å compared to the M06-2X/6-31G(d,p) values. The experimental hydrogen bond length in the case of $\mathbf{CC_M}$ dimer [18] agrees very well with ωB97X-D/6-31G(d,p) value, see Table 1. Additionally, in the case of M06-2X functional, inclusion of diffuse functions, i.e., M06-2X calculations using the 6-311+G(d,p) basis set, do not affect the dimerization energies and the geometries for a number of free amides and carboxylic acids heterodimers and homodimers with the exception of the hydrogen bond length of carboxylic acid dimers, where the addition of the

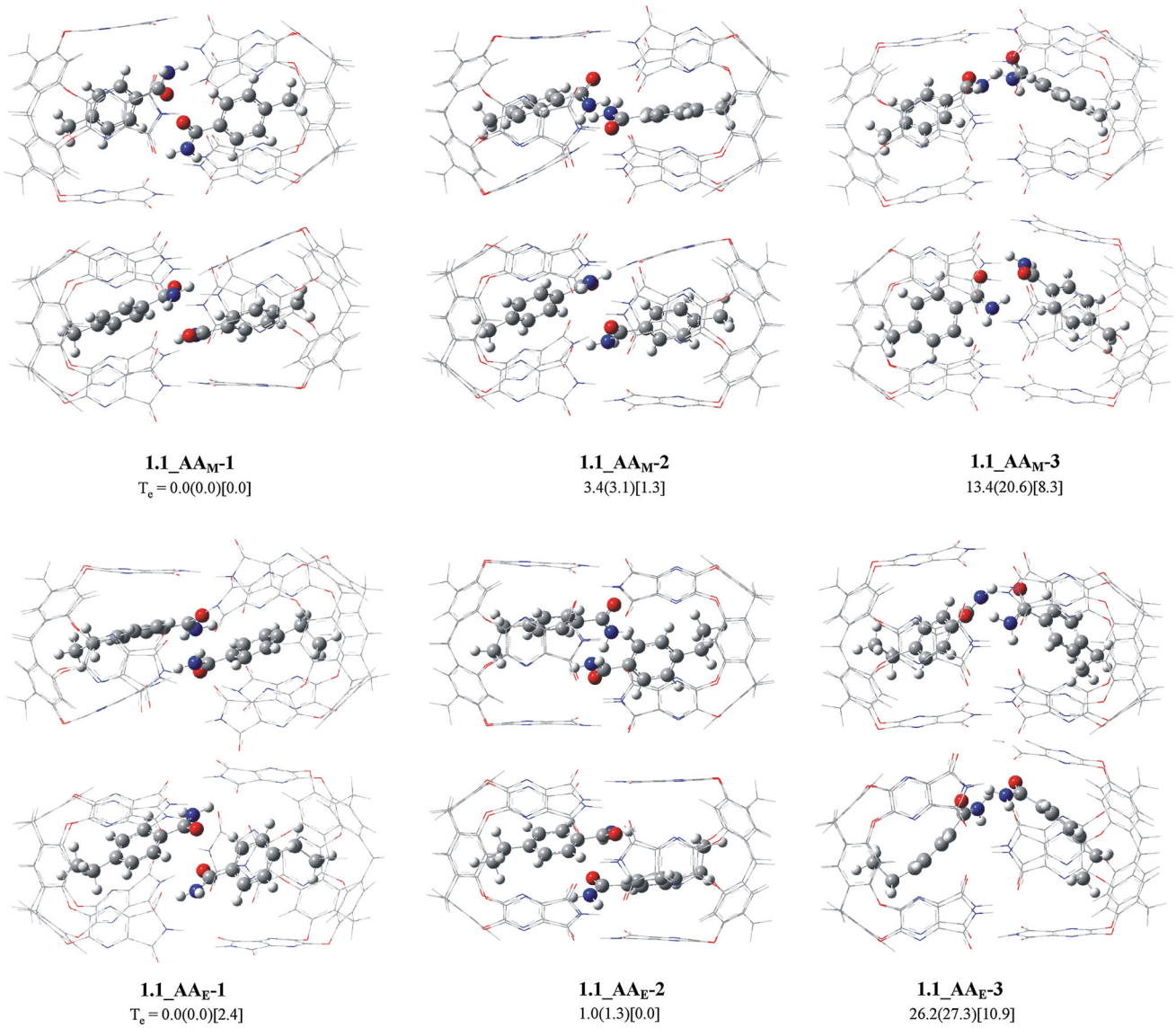

Fig. 2 Calculated structures of the lowest minima of the **1.1_AA$_M$** and **1.1_AA$_E$** species viewed from two different angles along with the corresponding T_e values, at the M06-2X/6-31G(d,p)(ωB97X-D/6-31G(d,p))[ONIOM:M06-2X/6-31G(d,p):PM6]. (H atoms = *white spheres*, C = *gray spheres*, O = *red spheres,* and N = *blue spheres*). The atoms of the capsule are designated with stick bonds for clarity

diffuse functions leads to elongated hydrogen bond distances. However, in the case of the encapsulated compressed dimers, **1.1_CC$_M$-1** and **1.1_CC$_E$-2** (see below), the elongation, due to the addition of the diffusion functions, is significantly reduced. It is calculated up to 0.03 Å, while all other geometries and dimerization energies are the same using both 6-31G(d,p) and 6-311+G(d,p) basis sets [23]. Thus, inclusion of diffuse functions, which increases greatly the computational effort, is not necessary for the purposes of the present work.

Regarding the dimerization energy of free dimers, the ωB97X-D/6-31G(d,p) method predicts larger dimerization energies by up to 1 kcal/mol. However, both M06-2X and ωB97X-D predict the same stability ordering for both *p*-methyl- and *p*-ethyl-substituted dimers, namely **CC>A-C>AA**. From the many-body decomposition energy, it seems that the deformation term (D), i.e., the energy penalty required to bring the monomers from their equilibrium geometries to the geometry of the dimer, is the smallest for the amide dimers and largest for the carboxylic acid dimers.

Thus, the larger dependence in M06-2X or ωB97X-D functionals and basis sets is observed only for the hydrogen bond distances of the free carboxylic acids. Both M06-2X/6-31G(d,p) and ωB97X-D/6-31G(d,p) levels of theory seem to be appropriate methods with the ωB97X-D/6-31G(d,p) level resulting in better agreement with experiment.

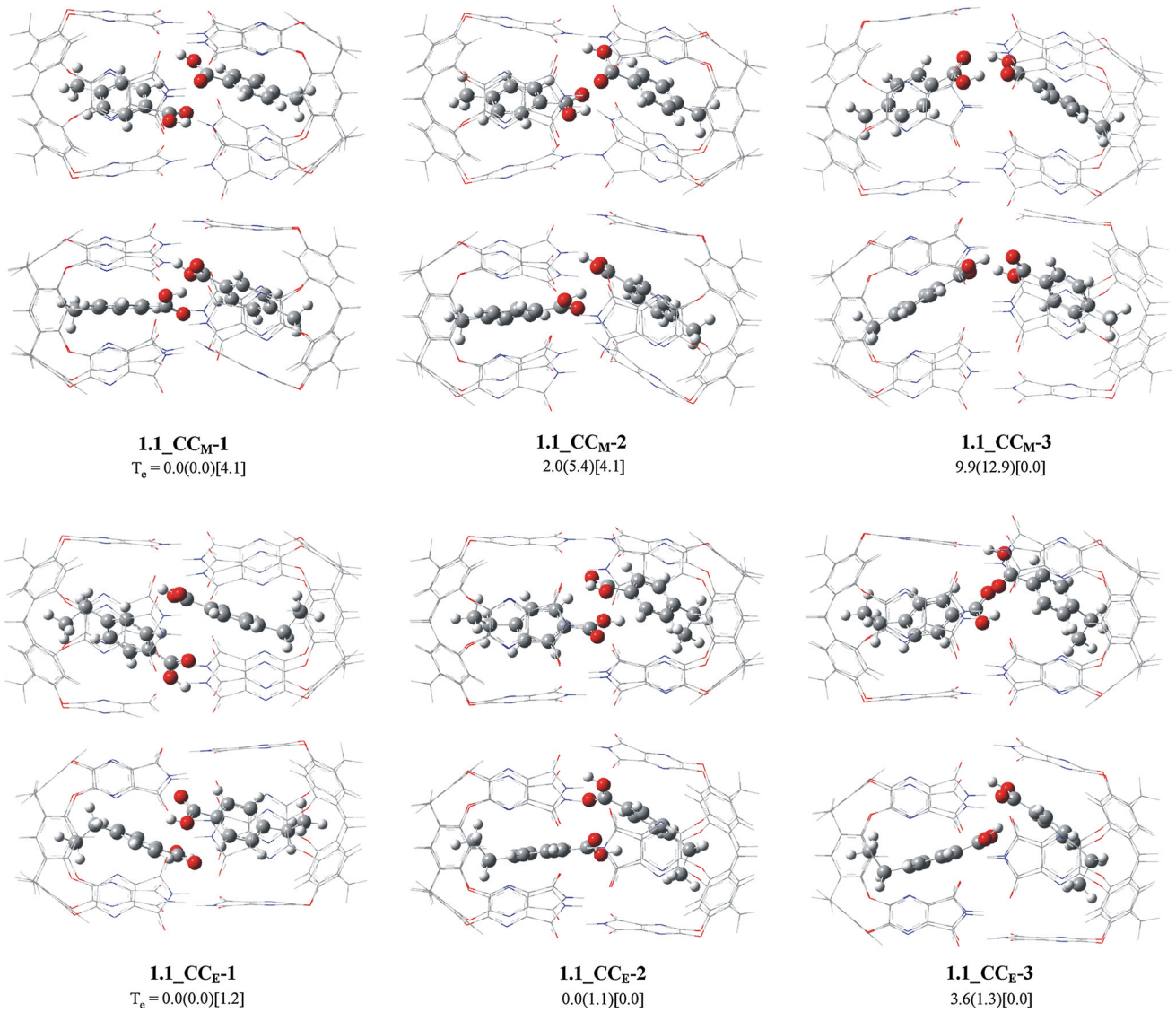

Fig. 3 Calculated structures of the lowest minima of the **1.1_CC$_M$** and **1.1_CC$_E$** species viewed from two different angles along with the corresponding T_e values, at the M06-2X/6-31G(d,p)(ωB97X-D/6-31G(d,p))[ONIOM:M06-2X/6-31G(d,p):PM6]. (H atoms = *white spheres*, C = *gray spheres*, O = *red spheres,* and N = *blue spheres*). The atoms of the capsule are designated with stick bonds for clarity

3.2 Encapsulated dimers

3.2.1 Geometry

The lowest two or three calculated minimum energy structures for each encapsulated complex are depicted in Fig. 2 for both methyl- and ethyl-substituted benzamide guests, in Fig. 3 for both substituted benzoic acid guests, and in Fig. 4 for both substituted benzamides–benzoic acids guests. The energy differences (T_e) from the lowest minimum structures in three levels of theory are given. Selected bond lengths, angles, and dihedral angles of the calculated encapsulated dimers are given in Table 2. The distances R_{2-3} and R_{6-7} correspond to the hydroxyl O–H or the amide N–H bond length and R_{3-4} and R_{7-8} corresponding to the hydrogen bond lengths (cf. numbering in Fig. 1). Of particular interest are the hydrogen bond distances between the cage and the monomers; the angles forming the hydroxyl bond or amide N–H bond and hydrogen bond lengths between monomers; the dihedral angles between the (8, 2, 3) and (4, 6, 7) planes for the dimers; and the dihedral angle between the two phenyl groups. The corresponding Cartesian coordinates of the calculated structures are given in the supporting information. In the free dimers, the ring formed by atoms 1–8 in Fig. 1 has the same geometry in both *p*-methyl and *p*-ethyl hetero- and homodimers, since they differ only in the R substituent at the para position of the benzoic acid and

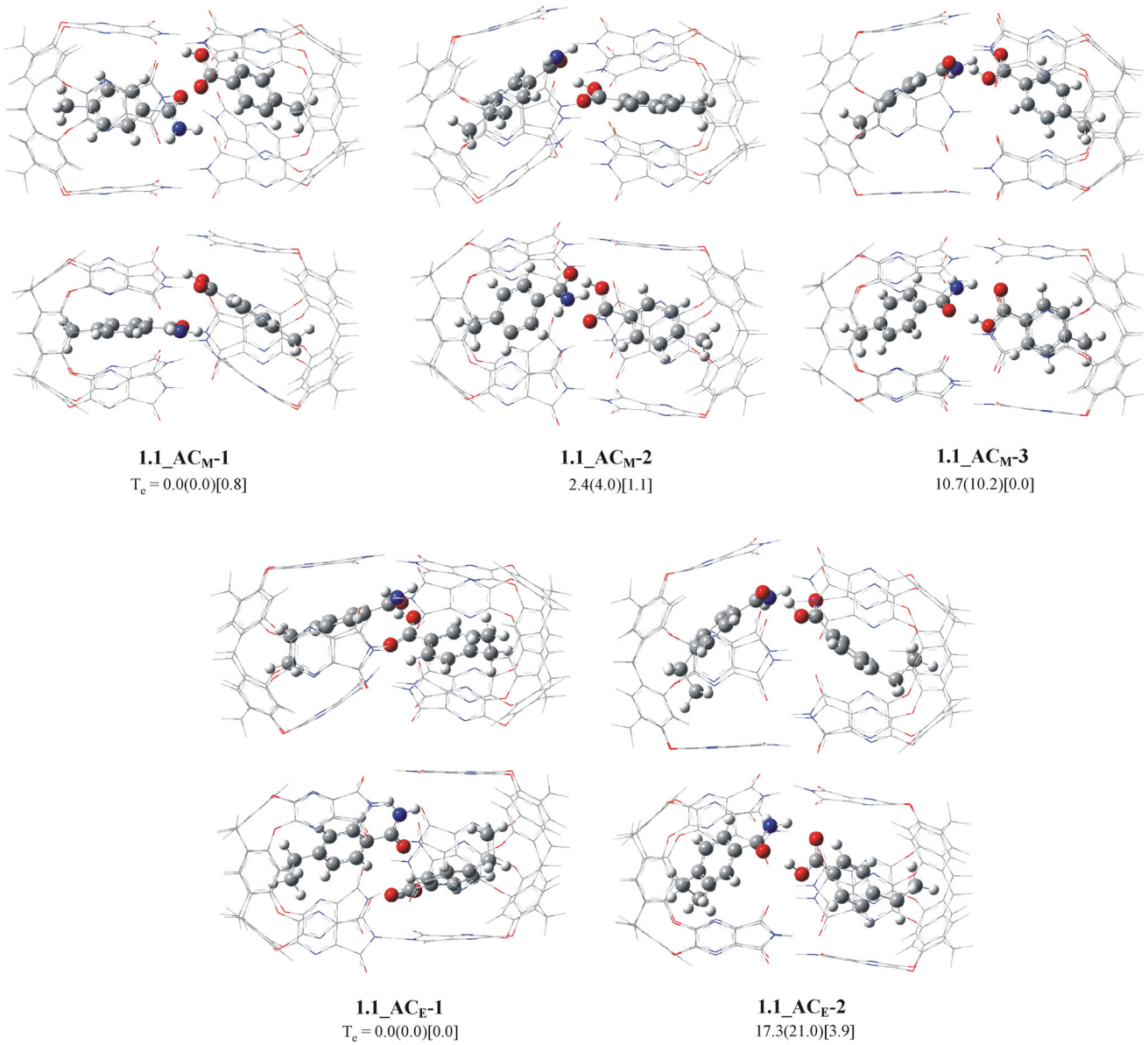

Fig. 4 Calculated structures of the lowest minima of the **1.1_AC$_M$** and **1.1_AC$_E$** species viewed from two different angles along with the corresponding T_e values, at the M06-2X/6-31G(d,p)(ωB97X-D/6-31G(d,p))[ONIOM:M06-2X/6-31G(d,p):PM6]. (H atoms = *white spheres*, C = *gray spheres*, O = *red spheres*, and N = *blue spheres*). The atoms of the capsule are designated with stick bonds for clarity

amide (Table 1). Upon encapsulation, the geometry of the ring and the relative position of the two monomers change significantly, due to the confined space within the cage and the guest–host interactions, compare Tables 1 and 2.

The M06-2X/6-31G(d,p) and ωB97X-D/6-31G(d,p) methods predict similar geometries for the minimum energy structures of the encapsulated complexes and the same relative energy ordering for their isomers. For some of these structures, some differences are observed mainly in the hydrogen bond lengths between monomers or monomers and the cage. The addition of diffuse functions for the encapsulated **1.1_CC$_M$-1** and **1.1_CC$_E$-2** structures, i.e., M06-2X/6-311+G(d,p)$_{dimers}$6-31G(d,p)$_{cage}$ level of theory, results in the same geometry as obtained with the M06-2X/6-31G(d,p). Thus, the diffuse functions do not affect the geometry of the present compressed encapsulated dimers. The ONIOM (M06-2X/6-31G(d,p):PM6) predicts the same minimum energy structures with similar geometries as obtained by the two full-DFT methodologies, see supporting information, but the ONIOM predicts a different energy ordering of the various isomers of the complexes in same cases and it seems that the calculated isomers of the complexes are more closely lying than the full-DFT methods see Figs. 2, 3, 4.

Table 1 Selected distances in Å, angles, and dihedral angles in degrees of the amide and carboxylic acid dimers and many-body decomposition of the calculated dimerization energies[a] ΔE in kcal/mol at the M06-2X (first entry) and ωB97X-D/6-31G(d,p) (second entry) levels of theory

Species	R_{1-2}	R_{2-3}	R^{b}_{3-4}	R_{4-5}	R_{5-6}	R_{6-7}	R^{b}_{7-8}	R_{8-1}	φ_{812}	φ_{234}	φ_{456}	φ_{678}	d^{c}_{1}	d^{d}_{2}	d^{e}_{3}	d^{f}_{4}	2-body[g]	D^{h}	ΔE
AA_M	1.346	1.025	1.855	1.233	1.346	1.025	1.855	1.233	122.9	176.4	122.9	176.4	0.0	0.0	21.1	21.1	−15.5	1.7	−13.9
	1.346	1.027	1.829	1.235	1.346	1.027	1.829	1.235	122.7	177.2	122.7	177.2	0.0	0.0	22.9	22.9	−16.7	1.8	−14.9
CC_M	1.308	1.014	1.557	1.232	1.308	1.014	1.557	1.232	123.8	179.5	123.8	179.5	0.1	0.2	0.1	0.1	−23.5	5.6	−17.9
	1.313	1.000	1.627	1.231	1.313	1.000	1.627	1.231	123.7	179.2	123.7	179.2	0.4	0.1	0.2	0.2	−22.6	4.0	−18.6
[i]		*0.992*	*1.636*			*0.992*	*1.636*												
AC_M	1.340	1.024	1.842	1.225	1.314	1.010	1.582	1.239	122.5	167.1	124.3	173.7	0.8	22.1	21.1	0.3	−19.7	3.5	−16.3
	1.342	1.025	1.827	1.226	1.315	1.003	1.625	1.239	122.3	169.0	124.3	173.6	0.7	21.9	22.5	0.2	−20.2	3.1	−17.1
AA_E	1.346	1.025	1.858	1.233	1.346	1.025	1.858	1.233	122.9	176.1	122.9	176.1	0.0	0.0	21.6	21.6	−15.5	1.7	−13.8
	1.346	1.027	1.829	1.235	1.346	1.027	1.829	1.235	122.7	177.3	122.7	177.3	0.0	0.0	23.3	23.3	−16.7	1.8	−14.9
CC_E	1.308	1.014	1.557	1.232	1.308	1.014	1.557	1.232	123.8	179.5	123.8	179.5	0.1	0.2	0.1	0.1	−24.8	7.0	−17.8
	1.313	1.000	1.629	1.231	1.313	1.000	1.625	1.231	123.7	179.3	123.7	179.3	0.4	0.1	0.2	0.2	−22.6	4.1	−18.5
AC_E	1.340	1.024	1.841	1.225	1.314	1.010	1.582	1.239	122.5	166.9	124.3	173.8	0.4	19.9	20.6	0.4	−19.7	3.4	−16.3
	1.342	1.025	1.829	1.226	1.315	1.003	1.624	1.239	122.3	169.0	124.3	173.5	0.4	23.0	22.5	0.6	−20.2	3.2	−17.1

[a] BSSE-corrected values

[b] Hydrogen bond distance between the two monomers

[c] Dihedral angle between the (8,2,3) and (4,6,7) planes for the dimers

[d] Dihedral angle between the two phenyl groups

[e] Dihedral angle between the (9,10,11) and (8,1,2) planes for the dimers

[f] Dihedral angle between the (12,13,14) and (6,5,4) planes for the dimers

[g] 2-Body: monomer–monomer interaction

[h] Deformation energy

[i] Experimental data, ref. 18; in CDF_3/CDF_2Cl solution 120 K

As shown in Figs. 2, 3, 4, all dimers in the **1.1** cage are highly compressed resulting in some isomers, having two monomers that interact very weak, or an unstable dimer, i.e., the encapsulated complex has two monomers instead of a dimer. In the cases where a dimer is formed, the cage slightly magnifies. In all isomers of the encapsulated complexes, the two monomers are not in the same plane. The lowest energy isomers of the six encapsulated complexes have one monomer lying above the other; while the calculated highest energy complexes of the six dimers have the two monomers forming a triangle, see Figs. 2, 3, 4. In all isomers, the monomers form hydrogen bonds with the walls of the capsule, except the **1.1_CC$_M$-3** isomer. These attractive interactions are responsible for the stabilization of the encapsulated complexes.

For both *p*-methyl and *p*-ethyl encapsulated substituted amides of **1.1_AA$_R$**, the two lowest structures are stabilized by hydrogen bonds, which are formed between the dimers and the cage and have bond lengths of 1.6–2.3 Å. Moreover, the second hydrogen atom of the amide group forms in addition to hydrogen bonds with the cage with lengths of 2.0–2.4 Å, resulting in an additional stabilization of the structures. It might be noted that the hydrogen bond distances between the two monomers are rather large, ranging from 3.2 to 3.7 Å, see Table 2, indicating a very weakened interaction. Thus, all six hydrogen and oxygen atoms of the two amide groups of the two monomers form stable hydrogen bonds with the cage. The angles N–H···O are about 70° for the *p*-methyl- and about 55° for the *p*-ethyl-substituted amide dimers instead of about 180 in the free dimer, see Table 2. Contrary to the above, in the third isomer of **1.1_AA$_R$**, hydrogen bonds between the two monomers are formed with bond lengths of 1.9–2.3 Å, see Table 2 and dimers are formed. Note that, in the free amide dimers, the hydrogen bond length is about 1.8 Å, see Table 1. Again, hydrogen bonds between the cage and the monomers are formed but not by all the hydrogen and oxygen atoms of the two amide groups. The angles N–H···O of dimers are about 150° (∼180 in the free dimer), and the dihedral angle between the two phenyl groups of the encapsulated dimer is about 50 (*p*-methyl-substituted dimer) and 80 (*p*-ethyl-substituted dimer) degrees instead of 0 in the free dimer, see Table 2.

Similarly to the amide encapsulated complexes above, the three isomers of the **1.1_CC$_E$** and the two lowest calculated isomers of the **1.1_CC$_M$** are stabilized by hydrogen bonds formed between the cage and the monomers, with lengths ≥1.7 Å. Only for the **1.1_CC$_E$-3** and **1.1_CC$_M$-3** isomers, carboxylic acids dimers are formed. In the **1.1_CC$_E$-3** isomer, a hydrogen bond between the monomers is formed of about 2.06 Å, while, in the **1.1_CC$_M$-3** isomer, two hydrogen bonds are formed between them, with bond lengths of 1.60 Å, which is similar to the corresponding hydrogen bond lengths in the free dimers. At the ωB97X-D/6-31G(d,p) level of theory, the **1.1_CC$_M$-3** isomer lies 13 kcal/mol above the lowest in energy isomer, and shorter hydrogen bond lengths between the two monomers are found than those of the free **CC** dimer. In this complex, the cage has slightly opened resulting in a small reduction in the compression and the formation of the dimer. Experimental studies on small compression of carboxylic dimers show a shortening of the hydrogen bond lengths [19]. Note that both functionals predict the same hydrogen bond length between the two monomers for the encapsulated **1.1_CC$_R$** complexes, while they differ about 0.07 Å in the free dimers, with the ωB97X-D value to be in very good agreement with the experiment, see Table 1. For all encapsulated complexes, the angles O–H···O of the dimer range from 55 to 90° (160° for **1.1_CC$_M$-3**) instead of about 180 in the free dimer. The dihedral angle between the two phenyl groups of the encapsulated monomers is about 30° (78° only for **1.1_CC$_M$-3**), see Table 2.

For the **1.1_AC$_E$** encapsulated structures, two stable isomers were calculated, and for **1.1_AC$_M$**, three stable minima were calculated. Again, for the lowest in energy **1.1_AC$_E$-1** and **1.1_AC$_M$-1**, the monomers are stable only due to the interaction with the walls of the capsule. In the remaining structures, **AC** dimers are formed. In the **1.1_AC$_E$-2** isomer, a hydrogen bond O–H···O between the monomers is formed of length about 1.7 Å. It is ∼0.1 Å larger than in the free **AC$_R$** dimer. Finally, for the **1.1_AC$_E$-2** and **1.1_AC$_M$-3** isomers, two hydrogen bonds, N–H···O and O–H···O, between the monomers are formed of about 1.9 and 1.6 Å length, while in free dimers the corresponding bond lengths are 1.8 and 1.6 Å, respectively. For these two encapsulated isomers, only the second hydrogen atom of the amide group forms hydrogen bond with an oxygen atom of the capsule with a bond length of about 2.0 Å. The dihedral angle between the two phenyl groups of the encapsulated monomers is about 30° for all encapsulated **1.1_AC** dimers with the exception of **1.1_AC$_E$-2** (81°), see Table 2. In the **1.1_AC$_M$-3** complex, which lies ∼10 kcal/mol above the lowest in energy isomer, shorter hydrogen bond lengths between the two monomers are found with respect to the free **AC** dimers. As in the case of the **1.1_CC$_M$-3** isomer, also in the **1.1_AC$_M$-3** complex, the cage is slightly magnified, the compression is reduced, and the formation of a dimer with a shortening of the hydrogen bond lengths is obtained.

3.2.2 *Energetics*

The calculated BSSE-corrected interaction energies of the encapsulated monomers inside the cage (listed under ΔE, ΔE = E(dimer) − 2E(monomer) + BSSE), the energy of the encapsulation of the dimers (listed under ΔE_1,

Table 2 Selected distances in Å, angles, and dihedral angles in degrees of the encapsulated amide and carboxylic acid dimers at the M06-2X/6-31G(d,p) (first entry) and ωB97-XD/6-31G(d,p) (second entry) levels of theory

Species	$R_{1\text{-}2}$	$R_{2\text{-}3}$	$R^{a}_{3\text{-}4}$	$R_{4\text{-}5}$	$R_{5\text{-}6}$	$R_{6\text{-}7}$	$R^{a}_{7\text{-}8}$	$R_{8\text{-}1}$	$R_{H\cdots Oc}$[b]	$R_{O\cdots Hc}$[c]	$R_{H\cdots Oc}$[b]	$R_{O\cdots Hc}$[c]	φ_{812}	φ_{234}	φ_{456}	φ_{678}	d_1[d]	d_2[e]	d_3[f]	d_4[g]
1.1_ AA_M-1	1.341	1.018	3.376	1.234	1.338	1.011	3.530	1.240	1.988,2006[i]	1.542	2.026,1.927[i]	1.909	123.5	63.1	121.9	76.5	17.5	8.1	25.7	19.1
	1.343	1.017	3.350	1.238	1.333	1.012	3.718	1.239	2.001,2.008[i]	1.585	1.964,1.892[i]	1.702	123.5	66.0	122.0	76.3	18.3	7.9	29.8	14.2
1.1_ AA_M-2	1.337	1.019	3.161	1.242	1.337	1.014	3.565	1.241	2.002,2.262[i]	1.616	2.306,2.031[i]	1.516	123.9	70.8	122.9	79.0	18.4	16.5	22.9	19.0
	1.338	1.018	3.190	1.240	1.339	1.013	3.674	1.241	1.982,2.258[i]	1.623	2.273,2.031[i]	1.547	123.4	72.4	122.8	76.7	16.3	15.9	23.6	20.7
1.1_ AA_M-3	1.352	1.017	1.921	1.236	1.339	1.017	2.266	1.229	2.065[i]		2.302,2.016[i]	2.139	123.6	149.1	122.9	115.7	85.3	64.0	24.6	28.1
	1.352	1.017	1.896	1.240	1.337	1.014	2.218	1.231	2.048[i]		2.608,1.993[i]	1.971	123.4	155.7	123.3	118.0	77.7	52.1	25.0	33.1
1.1_ CC_M-1	1.320	0.992	2.530	1.215	1.333	0.985	3.425	1.221	1.743	1.893	1.766	2.457	123.7	101.6	122.9	57.9	36.9	29.8	23.6	10.7
	1.317	0.989	2.888	1.217	1.328	0.989	3.593	1.222	1.765	1.815	1.695	2.850	123.3	89.9	123.0	58.4	28.9	30.3	25.8	5.3
[h]	1.319	0.990	2.560	1.210	1.331	0.983	3.460	1.216	1.749	1.899	1.761	2.469	112.7	118.0	109.8	80.1	37.7	29.9	23.2	10.7
1.1_ CC_M-2	1.319	0.991	2.937	1.222	1.327	0.983	1.876	1.224	1.720	2.402	2.808	1.835	123.2	76.6	123.1	134.4	48.4	39.1	20.0	5.8
	1.315	0.988	3.035	1.224	1.323	0.983	1.809	1.226	1.721	2.632	2.759	1.767	123.4	76.3	123.2	137.0	52.0	36.2	16.8	12.1
1.1_ CC_M-3	1.312	1.003	1.606	1.231	1.313	1.004	1.592	1.231					124.0	156.9	124.1	159.1	47.6	78.5	12.4	10.4
	1.312	0.999	1.594	1.231	1.312	0.999	1.598	1.231					123.9	160.3	123.9	160.0	58.9	78.1	6.8	7.6
1.1_ AC_M-1	1.334	1.014	2.773	1.217	1.325	0.989	3.158	1.247	2.196,2.139[i]	1.581	1.727	2.050	122.2	91.6	123.2	71.7	26.2	34.2	6.9	9.9
	1.340	1.014	2.892	1.222	1.318	0.987	3.190	1.244	2.181,1.970[i]	1.573	1.719	1.817	122.4	88.0	124.0	73.1	15.8	26.2	8.5	6.4
1.1_ AC_M-2	1.335	1.018	3.143	1.224	1.324	0.994	1.712	1.242	1.969,2.244[i]	2.406		1.826	122.3	72.8	123.1	145.6	58.3	43.4	28.6	9.4
	1.333	1.018	3.230	1.226	1.319	0.996	1.655	1.243	1.931,2.194[i]	2.530		1.778	122.3	72.8	123.3	146.7	59.7	40.3	30.7	14.0
1.1_ AC_M-3	1.334	1.021	1.884	1.227	1.314	1.021	1.510	1.247	2.114[i]				121.7	157.4	124.0	165.0	71.3	71.8	17.9	9.3
	1.334	1.015	2.072	1.223	1.320	1.002	1.581	1.248	1.892[i]				122.4	149.0	123.5	161.3	94.3	33.8	32.6	30.9
1.1_ AA_E-1	1.338	1.017	3.982	1.242	1.334	1.017	3.635	1.247	1.990,1.971[i]	1.777	1.897,1.993[i]	1.962	121.9	57.9	122.3	59.5	2.8	24.6	30.6	14.0
	1.343	1.017	3.973	1.241	1.332	1.015	3.859	1.240	2.061,2.045[i]	1.538	1.809,1.895[i]	1.833	123.3	56.5	121.8	53.0	6.1	17.0	26.0	10.3
1.1_ AA_E-2	1.351	1.010	4.621	1.228	1.359	1.011	3.546	1.230	2.277[i]	2.795	2.738,2.319[i]	2.356	122.9	48.9	122.5	52.5	23.0	36.8	32.5	27.2
	1.351	1.008	4.630	1.228	1.359	1.009	3.592	1.232	2.474[i]	3.087	2.438,2.205[i]	2.980	122.1	47.2	122.6	53.8	29.0	37.0	26.8	33.9
1.1_ AA_E-3	1.342	1.019	1.862	1.235	1.344	1.022	1.870	1.234	2.141[i]		2.584[i]		122.5	141.5	123.1	149.0	78.2	83.7	27.0	29.4
	1.341	1.019	1.855	1.235	1.344	1.021	1.834	1.236	2.069[i]		2.593[i]		122.6	146.6	122.6	145.4	76.8	84.5	30.2	23.2
1.1_ CC_E-1	1.336	0.990	5.162	1.213	1.341	0.970	4.293	1.214	1.734	2.574	2.746	2.675	123.2	50.0	122.9	55.3	35.5	37.0	2.9	8.7
	1.328	0.990	4.472	1.214	1.339	0.968	3.923	1.217	1.687	2.609	3.115	3.004	123.5	55.1	122.5	58.2	23.8	30.3	3.1	11.6
1.1_ CC_E-2	1.331	0.993	3.684	1.216	1.338	0.972	3.391	1.215	1.698	2.439	2.596[j]	2.588	123.6	56.6	122.8	73.3	32.2	33.5	22.0	23.1
	1.325	0.992	4.326	1.214	1.343	0.968	3.605	1.217	1.651	2.680	2.869[j]	3.032	123.9	56.5	122.6	66.4	28.1	29.7	18.9	22.5
[h]	1.331	0.989	3.717	1.120	1.338	0.970	3.476	1.209	1.709	2.444	2.563[j]	2.608	123.4	56.6	122.6	72.6	30.7	32.4	22.3	24.5
1.1_ CC_E-3	1.323	0.987	3.173	1.215	1.335	0.978	1.912	1.223	1.832	2.208	2.522	2.660	122.5	66.9	124.1	66.2	70.3	54.4	19.1	7.7
	1.342	0.968	3.636	1.217	1.325	0.992	2.063	1.214	1.653	2.690	2.743	2.964	124.0	56.8	122.4	66.2	27.4	29.9	19.2	23.5
1.1_ AC_E-1	1.358	1.014	5.118	1.223	1.319	0.986	3.161	1.228	2.295,2.211[i]		1.812	1.847	121.4	59.2	123.1	62.4	55.6	27.8	14.1	14.0
	1.356	1.011	5.204	1.225	1.316	0.986	3.266	1.229	2.289,2.310[i]		1.772	1.767	121.3	58.5	122.7	60.6	55.4	29.6	13.9	12.0
1.1_ AC_E-2	1.335	1.016	1.870	1.222	1.319	1.003	1.635	1.242	2.027[i]				122.0	138.7	124.4	153.6	74.1	81.9	22.4	26.2

Table 2 continued

Species	$R_{1\text{-}2}$	$R_{2\text{-}3}$	$R^{a}_{3\text{-}4}$	$R_{4\text{-}5}$	$R_{5\text{-}6}$	$R_{6\text{-}7}$	$R^{a}_{7\text{-}8}$	$R_{8\text{-}1}$	$R_{H^{\cdots}Oc}$[b]	$R_{O^{\cdots}Hc}$[c]	$R_{H^{\cdots}Oc}$[b]	$R_{O^{\cdots}Hc}$[c]	φ_{812}	φ_{234}	φ_{456}	φ_{678}	d^{d}_{1}	d^{e}_{2}	d^{f}_{3}	d^{g}_{4}
	1.337	1.016	1.863	1.223	1.317	0.997	1.630	1.242	2.010[i]				122.2	142.5	124.2	152.6	73.9	81.1	24.8	18.9

[a] Hydrogen bond distance between the two monomers

[b] Hydrogen bond distance between hydrogen atom of the monomers and oxygen atom of the cage

[c] Hydrogen bond distance between oxygen atom of the monomers and hydrogen atom of the cage

[d] Dihedral angle between the (8, 2, 3) and (4, 6, 7) planes of the dimers

[e] Dihedral angle between the two phenyl groups

[f] Dihedral angle between the (9, 10, 11) and (8, 1, 2) planes of the dimers

[g] Dihedral angle between the (12, 13, 14) and (6, 5, 4) planes of the dimers

[h] Ref. 10; M06-2X/6-311 + G(d,p):M06-2X/6-31G(d,p) for the dimer:cage

[i] The second H atom of the amide group, which does not interact with the O of the other monomer

[j] Distance between the carboxylic hydrogen atom of the monomer and the center of the phenyl group of the other monomer

ΔE_1 = E(encapsulated complexes) − E(cage) − E(dimer) + $BSSE_1$), the energy of the monomers (ΔE_2, ΔE_2 = E (encapsulated complexes) − E(cage) − 2E(monomer) + $BSSE_2$), and the energy with respect to the monomers and the full disassembled cage (ΔE_3, ΔE_3 = E(encapsulated complexes) − 2 E(**1**) − 2E(monomer) + $BSSE_3$) for all calculated isomers are given in Table 3. Note that the BSSE corrections are not the same for all interaction energies because they depend on the decomposition products. The many-body decomposition of the ΔE, ΔE_1, and ΔE_2 energetics for the lowest minimum of the each encapsulated dimer is given in Table 4.

As can be seen from Table 1, the two full-DFT computations for all isomers present similar ΔE values (interaction or dimerization energies of the encapsulated monomers inside the cage). Dimerization of the lowest energy encapsulated isomers (labeled as **–1**) is unfavorable (positive ΔE), while the third in energy order isomers (labeled as **–3**) and in three cases out of six, i.e., $\mathbf{AA_E}$, $\mathbf{AC_M}$, $\mathbf{AC_E}$, the second ones (**–2**) dimerization is favorable (negative ΔE). However, for all isomers, encapsulation is favored energetically due to the interactions between the dimer and the cage, see ΔE_1 values of Table 3, and these lead to the lowest energy structures.

Comparing the two M06-2X and ωB97X-D functionals, we observe that they predict the same relative energy ordering for the isomers of the encapsulated complexes, see above, almost the same dimerization energies of the free dimers and of the encapsulated dimers inside the cage, and the same interaction energy between the two cavitands **1** in the **1.1** cage, i.e., 57.5 and 57.1 kcal/mol for the M06-2X and ωB97X-D functionals, respectively. However, the two functionals present a difference in the energy of encapsulation of about 28 kcal/mol, namely the energies of the encapsulation of the dimers (ΔE_1) and of the monomers (ΔE_2) calculated via the ωB97X-D functional are larger than the corresponding M06-2X values, see Table 3. Given that the interaction energy between the two cavitands **1** in the **1.1** cage is the same for both functionals, similarly the ΔE_3 values differ also by the same amount. The larger encapsulation energy predicted by ωB97X-D compared to M06-2X arises from the fact that the ωB97X-D functional includes long-range corrections and empirical dispersions and calculates interactions between the guests and the cage with larger interaction energies than M06-2X. However, the important issue is that, even though the ΔE_1, ΔE_2, ΔE_3 values are larger with ωB97X-D than with M06-2X, both functionals predict that the lowest encapsulated complexes are stabilized via attractive interactions between the guests and the walls of the cage. These interactions are maximized by the compression of the dimer even though energy is needed for this purpose.

Table 3 Relative energy ordering T_e^a of the isomers, interaction energies[a,b] of the encapsulated guests inside the cage (ΔE, dimerization energies), and their interaction energies[a,b] with respect to the free cage and the dimers (ΔE_1), to the free cage and the monomers (ΔE_2), and to the four components of fully disassembled complexes (ΔE_3) at the M06-2X/6-31G(d,p) (first entry), ωB97X-D/6-31G(d,p) (second entry) ONIOM(M06-2X/6-31G(d,p):PM6) (third entry) and levels of theory

	R = Methyl					R = Ethyl				
	T_e	ΔE	ΔE_1	ΔE_2	ΔE_3^c	T_e	ΔE	ΔE_1	ΔE_2	ΔE_3^c
1.1_AA$_R$-1	0.0	2.8	−22.9	−37.1	−112.1 (−100.3)	0.0	4.2	−19.2	−32.9	−112.7 (−100.8)
	0.0	2.1	−54.4	−70.1	−143.0 (−133.4)	0.0	4.3	−47.6	−62.7	−136.2 (−126.6)
	0.0	−0.3				2.4	0.1			
1.1_AA$_R$-2	3.4	3.0	−17.8	−32.5	−108.8 (−96.9)	1.0	−3.7	−28.4	−41.6	−111.6 (−99.8)
	3.1	2.1	−50.8	−66.9	−139.9 (−130.4)	1.3	−4.0	−51.7	−66.5	−134.9 (−125.3)
	1.3	−1.5				0.0	−4.6			
1.1_AA$_R$-3	13.4	−2.7	−12.9	−26.6	−98.7 (−86.8)	26.2	−1.7	−0.6	−14.1	−86.4 (−74.6)
	20.6	−3.1	−37.2	−52.0	−122.3 (−112.8)	27.3	−3.1	−23.8	−38.6	−108.9 (−99.3)
	8.3	−7.8				10.9	−8.2			
1.1_CC$_R$-1[d]	0.0	1.9	−11.9	−30.0	−103.1 (−91.2)	0.0	2.1	−11.0	−29.6	−101.7 (−89.9)
	0.0	2.8	−41.2	−60.3	−131.9 (−122.3)	0.0	1.1	−38.6	−57.7	−127.1 (−117.5
	4.1	−0.6				1.2	−1.3			
1.1_CC$_R$-2	2.0	−2.1	−9.2	−27.0	−101.0 (−89.2)	0.0	0.4	−12.4	−30.2	−101.8 (−89.9)
	5.4	−0.5	−36.6	−55.3	−126.5 (−116.9)	1.1	1.3	−37.7	−56.4	−126.0 (−116.4)
	4.1	−0.6				0.0	−1.6			
1.1_CC$_R$-3	9.9	−11.3	−3.9	−21.3	−93.2 (−81.3)	3.6	−0.8	−8.5	−26.2	−98.1 (−86.3)
	12.9	−12.0	−30.6	−48.8	−119.0 (−109.4)	1.3	1.2	−37.5	−56.3	−125.8 (−116.3)
	0.0	−14.2				0.0	−3.6			
1.1_AC$_R$-1	0.0	0.9	−15.4	−32.4	−107.1 (−95.2)	0.0	3.5	−12.5	−29.1	−103.9 (−92.0)
	0.0	1.1	−44.7	−62.8	−135.4 (−125.8)	0.0	3.9	−42.1	−59.8	−131.7 (−122.2)
	0.8	−2.2				0.0	1.7			
1.1_AC$_R$-2	2.4	−4.5	−14.5	−30.6	−104.7 (−92.8)	17.3	−2.5	1.8	−14.2	−86.6 (−74.7)
	4.0	−3.1	−43.2	−60.2	−131.3 (−121.7)	21.0	−4.7	−23.4	−40.2	−110.7 (−101.2)
	1.1	−4.2				−3.9	−10.0			
1.1_AC$_R$-3	10.7	−9.6	−9.9	−25.8	−96.4 (−84.5)					
	10.2	−5.4	−37.4	−54.3	−125.2 (−115.6)					
	0.0	−12.5								

[a] In kcal/mol, BSSE-corrected values

[b] ΔE = E(dimer) − 2E(monomer) +BSSE; ΔE_1 = E(encapsulated complexes) − E(cage) − E(dimer) + $BSSE_1$; ΔE_2 = E(encapsulated complexes) − E(cage) − 2E(monomer) + $BSSE_2$; ΔE_3 = E(encapsulated complexes) − 2 E(**1**) − 2E(monomer) + $BSSE_3$

[c] Interaction energy with respect to the cavitands and spacers in the geometry of the capsule (with respect to the free cavitands and spacer)

[d] Ref. [23]

Both functionals predict the largest ΔE_1, ΔE_2, and ΔE_3 values for the **1.1_AA$_R$-1** and the smallest values for **1.1_CC$_R$-1**. The values of the lowest encapsulated dimers range from −39 to −54 (ΔE_1), from −58 to −70 (ΔE_2), and from −127 to −143 kcal/mol (ΔE_3) at the ωB97X-D/6-31G(d,p) level of theory, see Table 4. The high stability computed for the encapsulated complexes with respect to complete disassembling of the dimers and the cage might be noted. The analysis of the many-body interaction energy terms for the free dimers and the encapsulated complexes are presented in Tables 1 and 4, respectively. The size of the deformation term, D, i.e., energy penalty required to bring the fragments from their equilibrium geometries to the geometry of the complex, for each ΔE, ΔE_1, and ΔE_2 interaction energy depicts the size of the distortion of its fragments. For the case of the dimerization energies, ΔE, the 2-body term and the deformation term are similar for both functionals. Moreover, for all complexes except **1.1_AA$_E$**, the deformation term is similar for both functionals, and the differences in computed values of the ΔE_1, and ΔE_2 interaction energies with the two functionals arises from the 2-body term of the cage–dimer interaction for the ΔE_1 and the 2-body$_1$ and 2-body$_2$ terms of the cage–monomer interactions for the ΔE_2. The 2-body$_1$ and

Table 4 Many-body decomposition of the calculated interaction energies[a] of the guests inside the cage (ΔE), interaction energies[a] of the encapsulated complexes with respect to the free cage and the dimers (ΔE_1) and to the free cage and the monomers (ΔE_2), at the M06-2X (first entry) and ωB97X-D/6-3"1G(d,p) (second entry) levels of theory for the lowest minima of the encapsulated dimers

	Two monomers → encapsulated dimer			Cage + dimer → encapsulated complexes			Cage + two monomers → encapsulated complexes					
	2-Body	D	ΔE	2-Body	D	ΔE_1	2-Body$_1^b$	2-Body$_2^b$	2-Body$_3^b$	3-Body	D	ΔE_2
1.1_AA$_M$-1	−1.0	3.8	2.8	−74.3	51.4	−54.4	−36.1	−37.3	−1.4	−1.0	38.6	−37.1
	−1.6	3.7	2.1	−101.7	47.3	−11.9	−50.8	−50.3	−1.9	−0.5	33.5	−70.1
1.1_CC$_M$-1	−3.1	5.0	1.9	−57.8	45.9	−41.2	−26.0	−32.3	−3.4	0.5	31.1	−30.0
	−1.7	4.4	2.8	−82.9	41.7	−15.4	−46.5	−36.9	−1.8	0.5	24.4	−60.3
1.1_AC$_M$-1	−2.9	3.9	0.9	−66.9	51.5	−44.7	−37.8	−29.2	−3.3	0.1	37.7	−32.4
	−3.1	4.2	1.1	−89.3	44.6	−19.2	−48.9	−40.3	−3.3	−0.1	29.8	−62.8
1.1_AA$_E$-1	−1.5	5.7	4.2	−96.5	77.4	−47.5	−47.0	−48.5	−1.9	−1.0	65.5	−32.9
	−2.3	6.6	4.3	−104.8	57.3	−11.0	−50.3	−54.0	−2.6	−0.5	44.8	−62.6
1.1_CC$_E$-1	−0.3	2.4	2.1	−47.8	36.8	−38.6	−21.8	−26.0	−0.5	0.0	18.7	−29.6
	−1.6	2.7	1.1	−67.7	29.0	−12.4	−31.3	−36.4	−1.8	0.0	11.8	−57.7
1.1_AC$_E$-1	0.2	3.4	3.5	−65.1	52.6	−42.1	−33.7	−31.7	−0.3	0.3	36.3	−29.1
	0.5	3.4	3.9	−87.8	45.7	−42.1	−45.3	−42.9	0.1	0.4	28.0	−59.8

[a] In kcal/mol, BSSE-corrected values; ΔE = E(encapsulated dimer) − 2E(monomer) + BSSE; ΔE_1 = E(encapsulated complexes) − E(cage) − E(dimer) + $BSSE_1$; ΔE_2 = E(encapsulated complexes) − E(cage) − 2E(monomer) + $BSSE_2$

[b] 2-body$_1$: cage-first monomer interaction; 2-body$_2$: cage-second monomer interaction; 2-body$_3$: interaction between the two monomers

2-body$_2$ terms are up to −51 kcal/mol. The 2-body$_3$ term of the monomer–monomer interaction and the 3-body term are very small and almost the same for both functionals. In all cases, the 2-body$_3$ term stabilizes the complexes, with an energy of up to 3 kcal/mol. The deformation term of the ΔE_1 is larger than that of the ΔE_2 showing larger deformation of the dimers compared to that of the two monomers with respect to the free species. Only the **1.1_AA$_R$** complexes have a 3-body term (nonadditive component) that stabilizes the system. Finally, comparing the relative magnitudes of the monomer–host interactions (2-body$_1$ and 2-body$_2$ terms of ΔE_2), dimer–host interactions (2-body term of ΔE_1) and monomer–monomer interaction (2-body$_3$ term of ΔE_2), we found that the dimer–host interaction is about double of the monomer–host interactions, as expected, and that the monomer–monomer interactions are very small, namely less than 10 % than the corresponding monomer–host interactions.

Regarding the very fast ONIOM method, it predicts the same minimum energy structures as the two full-DFT methodologies. There are some differences between the results of the ONIOM approach and those of the full DFT regarding the energy ordering of the various isomers and the energy spacing between the complexes but generally ONIOM is found to be adequate for calculations on the present compressed systems, given the great difference in the required computational effort.

The stability ordering of the free dimers is determined as **CC>AC>AA** for both *p*-methyl- and *p*-ethyl-substituted compounds as can be seen by the ΔE interaction energies, Table 1. Similarly, for the encapsulated *p*-ethyl-substituted dimers in a large cavity [20], the stability ordering was calculated and was found experimentally to be **1.2$_4$.1_CC>1.2$_4$.1_AC>1.2$_4$.1_AA**, which is the same with the free dimers. In the present encapsulated complexes, the dimers are unstable due to the confined space of the cavity and the complexes are stabilized by the interactions between the guest molecules and the walls of the cage. Thus, their ordering is determined by the ΔE_2 or ΔE_3 interaction energies, i.e., interactions between the monomers and the cage or to the monomers and the full disassembled cage. Both interaction energies point out the stability ordering of **1.1_AA>1.1_AC>1.1_CC**.

Molecules that are confined in severely limited spaces behave quite differently than those in dilute solution; both guest and host adapt to each other to properly fill the space and stabilize the assembly [19]. Hydrogen-bonding preferences in the capsule are responsible for the selective recognition and catalysis of enzyme-binding pockets through hydrogen bonding. Reversible encapsulation has led to understanding of how molecules get in and out of the spaces, how chemical interactions are amplified, how unusual reaction pathways can emerge, and how reactive intermediates are stabilized [19]. These characteristics also apply to molecules that are compressed in a cavity. The attractive van der Waals interactions between the guests and the internal walls are significant. The inner walls wield an internal pressure on the guest and as a result here, the

dimer is not formed in the lowest structures, i.e., the two monomers coexist in the capsule and the attractive interactions are maximized.

Consequently, in a large cage, homodimers and heterodimers of amides and carboxylic acids are formed as in a solvent or in the gas phase [15, 20]. When the cavity is not large enough and the dimers are slightly compressed, encapsulation leads to shortening of the hydrogen bond [19, 22]. When the compression is increased, the hydrogen bonds are elongated and the dimers are weakened [22] and in large compression, they do not exist as dimers, as shown here, while the relative stability ordering of the encapsulated guests is changed from that in a capsule with adequate space for the accommodation of dimers. In the quest for the development of organic molecules, cages capable for molecular recognition, isolation of reactive species [15] and separation [36], encapsulation complexes are now tools of physical organic chemistry on the nanoscale.

4 Conclusions

DFT (M06-2X and ωB97X-D/6-31G(d,p)) calculations have been carried out on the encapsulation of heterodimers and homodimers of the *p*-methylbenzoic acid ($\mathbf{C_M}$), *p*-ethylbenzoic acid ($\mathbf{C_E}$), *p*-methylbenzamide ($\mathbf{A_M}$), and *p*-ethylbenzamide ($\mathbf{A_E}$) molecules in limited space provide by the **1.1** cage. The results of both full-DFT calculations are in agreement with respect to the geometry, the dimerization energies, and the relative ordering of the different isomers. The ωB97X-D ΔE_1, ΔE_2, ΔE_3 values are larger by the same amount than the corresponding M06-2X values, but both functionals predict that the lowest encapsulated complexes are stabilized via attractive interactions between the guests and the walls of the cage. The monomer–monomer interactions are less than 10 % of the corresponding monomer–host interactions. The monomer–host interactions are maximized by the destruction of the dimer even though energy is needed for this purpose. Thus, while the encapsulation is favorable even for the *p*-ethyl compounds, dimers are not formed inside the cage. This is the reason why the present encapsulated dimers have not been found experimentally. The dimers formed in the **1.1** encapsulated structures lie at >4 kcal/mol above the lowest minima. The isomerism of the encapsulated dimers arises from the different arrangements of small-molecule guests in the space of a self-assembled host. The guest dimers can adopt a different arrangement in the limited space of a self-assembled host than the most stable structure of the free dimers. Compression changes the relative stability of the encapsulated guests. For both free *p*-methyl- and *p*-ethyl-substituted compounds, the stability ordering is **CC>AC>AA**. The same relative stability of the guests in a large cavity was found too [20]. However, in the compressed encapsulated complexes, the stability ordering of the encapsulated complexes having two monomers is reversed to **1.1_AA>1.1_AC>1.1_CC**. This is an example of the possibility of separation of competitive monomers or dimers via reversible encapsulation under appropriate conditions.

Acknowledgments Financial support from GSRT and the EC through the European Fund for Regional Development, NSRF 2007–2013 action Development of Research Centers—KPHPIS, project "NewMultifunctional Nanostructured Materials and Devices—POLYNANO" to GT and IDP is acknowledged.

References

1. (1996) Comprehensive supramolecular chemistry. In: Atwood JL, Davies JED, MacNicol DD, Vögtle F, Lehn JM (eds) Supramolecular reactivity and transport: bioinorganic systems, vol 5. Pergamon, Oxford
2. Jeffrey GA (1997) An introduction to hydrogen bonding. Oxford University Press, Oxford
3. (2000) Recent theoretical and experimental advances in hydrogen bonded clusters. In: Xantheas SS. Kluwer Academic Publishers, NATO ASI Series C: Mathematical and Physical Sciences, vol 561
4. Desiraju GR, Steiner T (2001) The weak hydrogen bond in structural chemistry and biology. Oxford University Press, Oxford
5. Cram DJ, Cram JM (1994) Container molecules and their guests, monographs in supramolecular chemistry. In: Stoddart JF (Ed) Royal Society of Chemistry, vol 4, Cambridge
6. Sherman JC (1995) Tetrahedron 51:3395–3422
7. Rebek J, Jr (1996) Chem Soc Rev 96:255–264
8. Warmuth R (2000) J Incl Phenom Mol Recognit Chem 37:1–38
9. Fochi F, Jacopozzi P, Wegelius E, Rissanen K, Cozzini P, Marastoni E, Fisicaro E, Manini P, Fokkens R, Dalcanale E (2001) J Am Chem Soc 123:7539–7552
10. Kang J, Hilmersson G, Santamaría J, Rebek J Jr (1998) J Am Chem Soc 120:3650–3656
11. van Wageningen AMA, Timmerman P, van Duynhoven JPM, Verboom W, van Veggel FCJM, Reinhoudt DN (1997) Chem Eur J 3:639–654
12. Conn MM, Rebek J Jr (1997) Chem Rev 97:1647–1668
13. Jasat A, Sherman JC (1999) Chem Rev 99:931–967
14. MacGillivray LR, Atwood JL (1999) Angew Chem Int Ed 38:1018–1033
15. Hof F, Craig SL, Nuckolls C, Rebek J Jr (2002) Angew Chem Int Ed 41:1488–1508
16. Imaoka T, Kawana Y, Kurokawa T, Yamamoto K (2013) Nat Commun 4:2581
17. Ajami D, Dube H, Rebek J Jr (2011) J Am Chem Soc 133:9689–9691
18. Ajami D, Tolstoy PM, Dube H, Odermatt S, Koeppe B, Guo J, Limback HH, Rebek J Jr (2011) Angew Chem Int Ed 50:528–531
19. Jiang W, Tiefenbacher K, Ajami D, Rebek J Jr (2012) Chem Sci 3:3022–3025
20. Tzeli D, Theodorakopoulos G, Petsalakis ID, Ajami D, Rebek J Jr (2011) J Am Chem Soc 133:16977–16985
21. Tzeli D, Petsalakis ID, Theodorakopoulos G, Ajami D, Rebek J Jr (2013) Int J Quant Chem 113:734–739

22. Tzeli D, Petsalakis ID, Theodorakopoulos G, Ajami D, Jiang W, Rebek J Jr (2012) Chem Phys Lett 548:55–59
23. Tzeli D, Petsalakis ID, Theodorakopoulos G (2013) Chem Phys Lett 573:48–55
24. Heinz T, Rudkevich DM, Rebek J Jr (1998) Nature 394:764–766
25. Zhao Y, Truhlar DG (2008) Theor Chem Acc 120:215–241
26. Zhao Y, Truhlar DG (2008) Acc Chem Res 41:157–167
27. Chai JD, Head-Gordon M (2008) Phys Chem Chem Phys 10:6615
28. Curtiss LA, McGrath MP, Blaudeau JP, Davis NE, Binning RC Jr, Radom L (1995) J Chem Phys 103:6104–6113
29. Tzeli D, Petsalakis ID, Theodorakopoulos G (2011) Phys Chem Chem Phys 13:11965–11975
30. Dapprich S, Komáromi I, Byun KS, Morokuma K, Frisch MJ (1999) J Mol Struct (Theochem) 462:1–21
31. Vreven T, Morokuma K, Farkas Ö, Schlegel HB, Frisch MJ (2003) J Comp Chem 24:760–769
32. Vreven T, Morokuma K (2006) Ann Rep Comp Chem 2:35–50
33. Boys SF, Bernardi F (1970) Mol Phys 19:553–566
34. Xantheas SS (1994) J Chem Phys 104:8821–8824
35. Frisch MJ, Trucks GW, Schlegel HB, Scuseria GE, Robb MA, Cheeseman JR, Scalmani G, Barone V, Mennucci B, Petersson GA, Nakatsuji H, Caricato M, Li X, Hratchian HP, Izmaylov AF, Bloino J, Zheng G, Sonnenberg JL, Hada M, Ehara M, Toyota K, Fukuda R, Hasegawa J, Ishida M, Nakajima T, Honda Y, Kitao O, Nakai H, Vreven T, Montgomery JA Jr., Peralta JE, Ogliaro F, Bearpark M, Heyd JJ, Brothers E, Kudin KN, Staroverov VN, Kobayashi R, Normand J, Raghavachari K, Rendell A, Burant JC, Iyengar SS, Tomasi J, Cossi M, Rega N, Millam NJ, Klene M, Knox JE, Cross JB, Bakken V, Adamo C, Jaramillo J, Gomperts R, Stratmann RE, Yazyev O, Austin AJ, Cammi R, Pomelli C, Ochterski JW, Martin RL, Morokuma K, Zakrzewski VG, Voth GA, Salvador P, Dannenberg JJ, Dapprich S, Daniels AD, Farkas Ö, Foresman JB, Ortiz JV, Cioslowski J, Fox DJ (2009) Gaussian Inc., Wallingford CT, Gaussian 09, Revision A1
36. Mitra T, Jelfs KE, Schmidtmann M, Ahmed A, Chong SY, Adams DJ, Cooper AI (2013) Nat Chem 5:276–281